



Selectively catalytic oxidation of 1,2-propanediol to lactic, formic, and acetic acids over Ag nanoparticles under mild reaction conditions



Yonghai Feng^{a,b}, Hengbo Yin^{a,*}, Aili Wang^a, Wuping Xue^a

^a Faculty of Chemistry and Chemical Engineering, Jiangsu University, Zhenjiang 212013, China

^b School of Material Science and Engineering, Jiangsu University, Zhenjiang 212013, China

ARTICLE INFO

Article history:

Received 22 January 2015

Revised 7 March 2015

Accepted 9 March 2015

Keywords:

1,2-Propanediol oxidation

Ag nanoparticles

Lactic acid

Formic acid

Acetic acids

Kinetics

ABSTRACT

Selectively catalytic oxidation of 1,2-propanediol with O₂ to lactic, formic, acetic acids over Ag nanoparticles was investigated. Ag nanoparticles and alkali cocatalyzed the oxidation of 1,2-propanediol. The Ag nanoparticles with the average particle sizes of 15.2–43.2 nm were prepared by using citric acid (CA), sodium dodecylbenzenesulfonate, tween-80 (Tween), D-sorbitol, and polyvinylpyrrolidone as organic modifiers. When the oxidation of 1,2-propanediol was catalyzed by Ag^{Tween} nanoparticles at 120 °C for 4 h in NaOH solution, the lactic acid selectivity was 62% at the 1,2-propanediol conversion of 65.6% while over Ag^{CA} nanoparticles, the acetic and formic acids selectivities were 63.2% and 30.5%, respectively, at the complete conversion of 1,2-propanediol. The small-sized Ag nanoparticles favored the formation of acetic and formic acids while the Ag nanoparticles with the average particle sizes of 19.4–25.3 nm favored the formation of lactic acid. The Ag nanoparticle sizes also affected the kinetics for the catalytic oxidation of 1,2-propanediol.

© 2015 Elsevier Inc. All rights reserved.

1. Introduction

Acetic acid with an annual production of more than 10 million tons worldwide is mainly produced by methanol carbonylation through the BP-Monsanto Cativa process over Rh (Ir) complex catalyst with iodide as a cocatalyst at 180–220 °C and 3–4 MPa [1,2]. The raw material, methanol, is produced from syngas, which is produced *via* steam reforming of natural gas or coal at *ca.* 800 °C [3–6]. The conventional production process for acetic acid not only uses non-renewable energy source but also uses expensive noble metals as the catalysts. Formic acid widely used in food, leather, and medical fields is commercially produced by the sodium formate method, in which carbon monoxide reacts with sodium hydroxide at 160–200 °C and 2 MPa, or by the methanol carbonylation method, in which methanol first reacts with carbon monoxide to produce methyl formate and, then, methyl formate is hydrolyzed to formic acid and methanol [7–10]. The raw materials, carbon monoxide and methanol, are derived from non-renewable fossil fuels. Lactic acid can be used for the synthesis of biodegradable polylactic acid and resin [11,12]. The global consumption of lactic acid is *ca.* 150,000 ton and is expected to increase rapidly in the near future [13,14]. Lactic acid is mainly produced by the

fermentation of carbohydrate. The fermentation process has disadvantages, such as large amount of water spending, low reaction rate, and high cost [15]. Additionally, biological sludge is unavoidably produced in the fermentation of carbohydrate.

In view of environmental issues and diminishing fossil fuel reserves, the production of chemicals from renewable biomass has attracted considerable interest [16–18]. 1,2-Propanediol derived from biomass-based polyols including glycerol and sorbitol *via* hydrogenolysis [17–21] has been now considered as an alternative and renewable carbon source for the synthesis of many highly value-added chemicals, such as lactic acid [22–29], pyruvic acid [30], acetic acid [22–25,27–29], formic acid [22–25,27–29], hydroxyacetone [24], propionic acid [31], and propanol [31], *via* either catalytic oxidation or bioconversion processes. However, 1,2-propanediol is facing the oversupply problem, especially in China, due to its limited demand in the production of organic solvent and unsaturated polyester resin [32,33] and the scaling-up coproduction of dimethyl carbonate and 1,2-propanediol by transesterification method [34]. In this case, investigation of renewable 1,2-propanediol oxidation to value-added lactic, formic, and acetic acids is highlighted.

Recently, research effort has mainly focused on the catalyst development for selective oxidation of 1,2-propanediol to lactic acid [22–29]. Prati et al. [22] reported that the 1,2-propanediol conversion and the lactic acid selectivity were 80% and 100%,

* Corresponding author. Fax: +86 (0)511 88791800.

E-mail address: yin@ujs.edu.cn (H. Yin).

respectively, when the oxidation of 1,2-propanediol was catalyzed by 1%Au/C catalyst at 90 °C and 0.3 MPa O₂. Xu et al. [29] found that the 2.8%Au/MgO catalyst showed high catalytic activity in the 1,2-propanediol oxidation reaction, giving the 1,2-propanediol conversion of 94.4%, lactic acid selectivity of 89.3%, and acetic acid selectivity of 10.7% under 0.3 MPa O₂ at 60 °C. Hutchings et al. [23,25] and Medlin et al. [26] have studied the oxidation of 1,2-propanediol over carbon-supported Au–Pd and Au–Pt bimetallic catalysts. As compared to the monometallic catalysts, the bimetallic catalysts showed high catalytic activity in the oxidation reaction. The 1,2-propanediol conversion and lactic acid selectivity were more than 94% and 95%, respectively, under 1 MPa O₂ at 60 °C. Our previous work [27] reported that 1,2-propanediol could be selectively oxidized to lactic acid over hydroxylapatite nanorod-supported Au–Pd catalyst at 80 °C under atmospheric pressure, giving the lactic acid selectivity of 97.1% at the 1,2-propanediol conversion of 96.6%. The previous work reveals that supported Au, Pd, and Pt monometallic or bimetallic catalysts have high catalytic activities in the oxidation of 1,2-propanediol to lactic acid with O₂ in an alkaline medium. However, the selectivities of acetic acid and formic acid were low over these supported noble metal catalysts.

Hutchings et al. [24] found that high acetic acid selectivity of 66% at the 1,2-propanediol conversion of 82% was obtained when the oxidation of 1,2-propanediol was catalyzed over Au–Pd/C catalyst in the absence of alkali under 0.3 MPa O₂ at 115 °C for 24 h. Acetic acid and lactic acid could be produced by the catalytic oxidation of 1,2-propanediol over supported noble metal catalysts under mild reaction conditions, but the formic acid selectivity was low.

The previous work focused on the catalytic activities of noble metals, such as Au, Pd, and Pt, for the oxidation of 1,2-propanediol. However, to the best of our knowledge, Ag with low cost has not been used as the catalyst for the oxidation reaction.

In our present work, lactic, acetic, and formic acids were selectively produced through the catalytic oxidation of 1,2-propanediol over Ag nanoparticles with different particle sizes in NaOH aqueous solution. Different-sized Ag nanoparticles were prepared by the wet chemical reduction method in the presence of different-structured organic modifiers. The Ag nanoparticle size played an important role in the selectively catalytic oxidation of 1,2-propanediol. A power-function type reaction kinetic model was used to estimate the oxidation kinetics of 1,2-propanediol over Ag nanoparticle catalysts. The recycling performances of Ag nanoparticle catalysts were also investigated.

2. Experimental

2.1. Materials

The chemicals, 1,2-propanediol, lactic acid, formic acid, acetic acid, hydroxyacetone, pyruvaldehyde, methanol, ethanol, *iso*-propanol, *n*-propanol, hydrazine hydrate (N₂H₄·H₂O), sodium hydroxide (NaOH), silver nitrate (AgNO₃), tween-80 (Tween), polyvinylpyrrolidone (PVP, K90), sodium dodecyl-benzenesulfonate (SDBS), *D*-sorbitol (DS), and citric acid, (CA) were of reagent grade and were purchased from Sinopharm Chemical Reagent Co., Ltd. All the chemicals were used as received without further purification.

2.2. Preparation of Ag nanoparticles

Ag nanoparticles were prepared by reducing silver nitrate with hydrazine hydrate in the presence of organic modifiers, such as CA, SDBS, Tween, PVP, and DS (Table 1). Typically, organic modifier

(0.05 g) and silver nitrate (1 g) were dissolved in distilled water (100 mL) by ultrasonic treatment for 30 min. Then, a hydrazine hydrate aqueous solution (3.0 mL in 100 mL water) was added dropwise to the mixture at 30 °C for 2 h under mild stirring. The resultant Ag nanoparticles were centrifuged and washed with anhydrous ethanol and distilled water for 3 times, respectively.

2.3. Characterization

The identification of crystal phases of Ag nanoparticles was performed by X-ray powder diffraction (XRD), which were recorded on a diffractometer (D8 super speed Bruke-AEX Company, Germany) with Cu K α ($\lambda = 1.54056 \text{ \AA}$) radiation in the range of 10–90°. The crystallite sizes of metallic silver, (111) plane, in Ag nanoparticles were calculated by using Scherrer's equation: $D = K\lambda / (B \cos \theta)$, where K was taken as 0.89 and B was the full width of the diffraction line at half of the maximum intensity. The crystallite sizes of Ag (111) are listed in Table 1.

The microstructures of Ag nanoparticles were examined by transmission electron microscopy (TEM) on a microscope (JEM-2100) operated at an acceleration voltage of 200 kV. The TEM specimens were prepared by placing a drop of Ag nanoparticle ethanol suspension onto a copper grid coated with a layer of amorphous carbon. The average particle sizes of the Ag nanoparticles were measured from the TEM images by counting at least 200 individual particles. The average particle sizes of Ag nanoparticles were calculated by a weighted-average method according to the individual particle sizes of all the counted particles.

2.4. Catalytic test

The catalytic reaction was performed in a 1000 mL stainless steel autoclave equipped with a magnetic stirrer. The appointed amounts of 1,2-propanediol, water, sodium hydroxide, and catalyst were added into the autoclave. Firstly, the autoclave was purged with N₂ for 10 min. After the given temperature was reached, O₂ was pressurized into the desired pressure and the oxidation of 1,2-propanediol started. After reacting for a certain time, the autoclave was cooled to ambient temperature and depressurized for product analysis.

The concentration of remained 1,2-propanediol was analyzed on a gas phase chromatograph equipped with a PEG-20 M packed capillary column (0.25 mm \times 30 m) and FID by the internal standard method with *n*-butanol as the internal standard. Before product analysis, the reaction mixture was acidified with hydrochloric acid (12 M) to the pH value of *ca.* 3. Lactic acid, acetic acid, and formic acid were the products detected and analyzed on a Varian HPLC system equipped with a reverse-phase column (Chromspher 5 C18, 4.6 mm \times 250 mm) and a UV detector ($\lambda = 210 \text{ nm}$) at 35 °C. The aqueous solution of H₃PO₄/NaH₂PO₄ (0.1 M NaH₂PO₄ acidified by H₃PO₄ to pH = 2) buffer aqueous solution and acetonitrile (*v:v* = 9:1) was employed as the eluent, and the flow rate was 0.6 mL min⁻¹. The concentrations of the products were analyzed by the external standard method. The selectivities of products were calculated on carbon basis.

3. Results and discussion

3.1. XRD analysis

The XRD patterns of Ag nanoparticles prepared in the presence of organic modifiers are shown in Fig. 1. When using PVP, DS, Tween, CA, and SDBS as modifiers, XRD peaks appearing at $2\theta = 38.1, 44.3, 64.4, 77.5, \text{ and } 81.5^\circ$ were indexed as the (111), (200), (220), (311), and (222) planes of the face-centered cubic

Table 1
Oxidation of 1,2-propanediol catalyzed by Ag nanoparticles prepared with different organic modifiers.^a

Catalysts	Organic modifiers	Average particle sizes ^b (nm)	Crystallite sizes of Ag (111) ^c (nm)	1,2-Propanediol conversions (%)	Selectivities (%)			TOF ^d (h ⁻¹)
					Lactic acid	Formic acid	Acetic acid	
Ag _{CA}	CA	15.2	14.8	100	6.3	30.5	63.2	25.2
Ag _{SDBS}	SDBS	19.4	17.6	81.9	48.1	17.6	35.3	20.6
Ag _{Tween}	Tween	25.3	23.2	65.6	62.0	13.8	24.2	16.5
Ag _{DS}	DS	33.6	30.6	58.8	27.4	23.8	48.8	14.8
Ag _{PVP}	PVP	43.8	40.1	42.6	35.4	22.1	42.5	10.7

^a Reaction conditions: 1,2-propanediol concentration, 0.28 mol L⁻¹; NaOH concentration, 0.56 mol L⁻¹; volume of solution, 200 mL; catalyst, 0.06 g; reaction temperature: 120 °C; reaction time: 4 h; and stirring rate, 600 rpm.

^b The average particle sizes of Ag nanoparticles were calculated by TEM.

^c The crystallite sizes of Ag (111) were calculated by XRD.

^d TOF = Conversion of 1,2-propanediol (mole) divided by the amount of metallic Ag (mole) and reaction time.

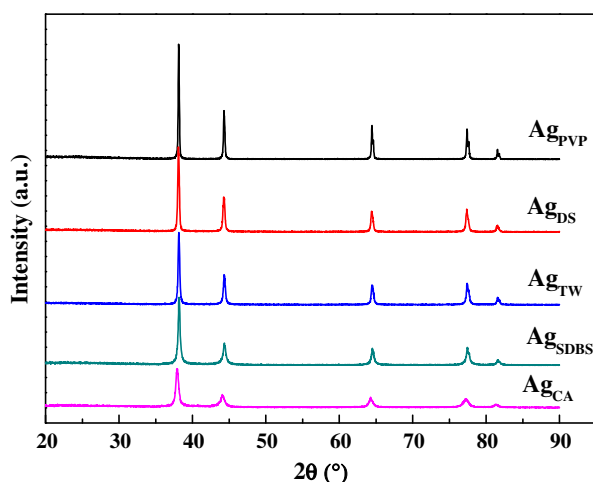


Fig. 1. XRD patterns of Ag nanoparticles prepared with CA, SDBS, Tween, DS, and PVP as organic modifiers.

(fcc) silver (JCPDS 46-1043). No diffraction peaks of silver oxides were detected, indicating that phase-pure metallic Ag nanoparticles were prepared under our present experimental conditions.

The crystallite sizes (111) of Ag nanoparticles were estimated by the Scherrer's equation (Table 1). As shown in Table 1, the crystallite sizes of the Ag nanoparticles ranged from 14.8 to 40.1 nm. The crystallite sizes were in an order of Ag_{CA} (14.8 nm) < Ag_{SDBS} (17.6 nm) < Ag_{Tween} (23.2) < Ag_{DS} (30.6 nm) < Ag_{PVP} (40.1 nm). The results revealed that there were different interactions between organic modifiers and silver precursor, giving different crystallite sizes of the as-prepared Ag nanoparticles.

3.2. TEM analysis

TEM images show that sphere-like Ag nanoparticles were prepared by using CA, SDBS, Tween, DS, and PVP as the organic modifiers, respectively (Fig. 2a, c, e, g, and i). According to the SAED and HRTEM analysis (Fig. 2b, d, f, h, and j), the as-prepared Ag nanoparticles were face-centered cubic (fcc) silver and had polycrystalline structure. When CA, SDBS, Tween, DS, and PVP were used as the organic modifiers, the average particle sizes and size distributions were 15.2, 5.0–25.0; 19.4, 6.3–50; 25.3, 5.8–58.8; 33.6, 23.1–46.2; and 43.8, 31.3–150.0 nm, respectively. The TEM analysis indicated that different-structured organic modifiers significantly affected the particle sizes of the as-prepared Ag nanoparticles. The average particle sizes were in an order of Ag_{CA} (15.2 nm) < Ag_{SDBS} (19.4 nm) < Ag_{Tween} (25.3 nm) < Ag_{DS} (33.6 nm) < Ag_{PVP} (43.8 nm), which was consistent with the result of XRD.

3.3. Oxidation of 1,2-propanediol catalyzed by Ag nanoparticles

The catalytic oxidation of 1,2-propanediol over Ag nanoparticles was carried out in NaOH aqueous solution at 120 °C and 1 MPa O₂ for 4 h. The results are listed in Table 1. When the Ag nanoparticles prepared by using CA as the organic modifier were used as the catalysts, the conversion of 1,2-propanediol was 100% and the selectivities of lactic acid, formic acid, and acetic acid were 6.3%, 30.5%, and 63.2%, respectively. When the Ag nanoparticles prepared by using SDBS and Tween as organic modifiers were used as the catalysts, the conversions of 1,2-propanediol were 81.9% and 65.3%, respectively and the selectivities of lactic acid, formic acid, and acetic acid were 48.1%, 17.6%, and 35.3%; 62.0%, 13.8%, and 24.2%. When the spherical Ag nanoparticles prepared by using DS and PVP as organic modifiers were used as the catalysts, the conversions of 1,2-propanediol were 58.8% and 42.6% and the selectivities of lactic acid, formic acid, and acetic acid were 27.4%, 23.8%, and 48.8%; 35.4%, 22.1%, and 42.5%, respectively.

According to the 1,2-propanediol conversions and TOF values, it was found that the oxidation rates of 1,2-propanediol over Ag nanoparticles were in an order of Ag_{CA} (15.2 nm) > Ag_{SDBS} (19.4 nm) > Ag_{Tween} (25.3 nm) > Ag_{DS} (30.6 nm) > Ag_{PVP} (43.8 nm). Small-sized Ag nanoparticles had higher catalytic activity for the oxidation of 1,2-propanediol than large-sized ones, favoring the formation of acetic acid and formic acid. Ag_{SDBS} and Ag_{Tween} nanoparticles with the average sizes of 19.4 and 25.3 nm, respectively, favored the formation of lactic acid. From the TEM images, it was found that the particle number percentages of Ag_{CA}, Ag_{SDBS}, and Ag_{Tween} nanoparticles with the particle sizes of less than 20 nm were 85.0%, 73.6%, and 41.0%, respectively. The lactic acid selectivities increased with the decrease in the particle number percentages of the Ag nanoparticles with the particle sizes of less than 20 nm. However, with the further increase in Ag particle sizes for Ag_{DS} and Ag_{PVP} nanoparticles, both 1,2-propanediol conversion and lactic acid selectivity decreased. It could be concluded that the oxidation of 1,2-propanediol to lactic acid was affected by the silver nanoparticle size.

3.4. Catalytic oxidation of 1,2-propanediol to lactic acid

Considering Ag_{Tween} nanoparticles had high catalytic activity for selective oxidation of 1,2-propanediol to lactic acid, it was selected as the model catalyst for investigating the effect of other reaction parameters on lactic acid formation.

3.4.1. Effect of reaction temperature

Fig. 3 shows the conversions of 1,2-propanediol and the selectivities of lactic acid, acetic acid, and formic acid in the oxidation of 1,2-propanediol catalyzed by Ag_{Tween} nanoparticles at different

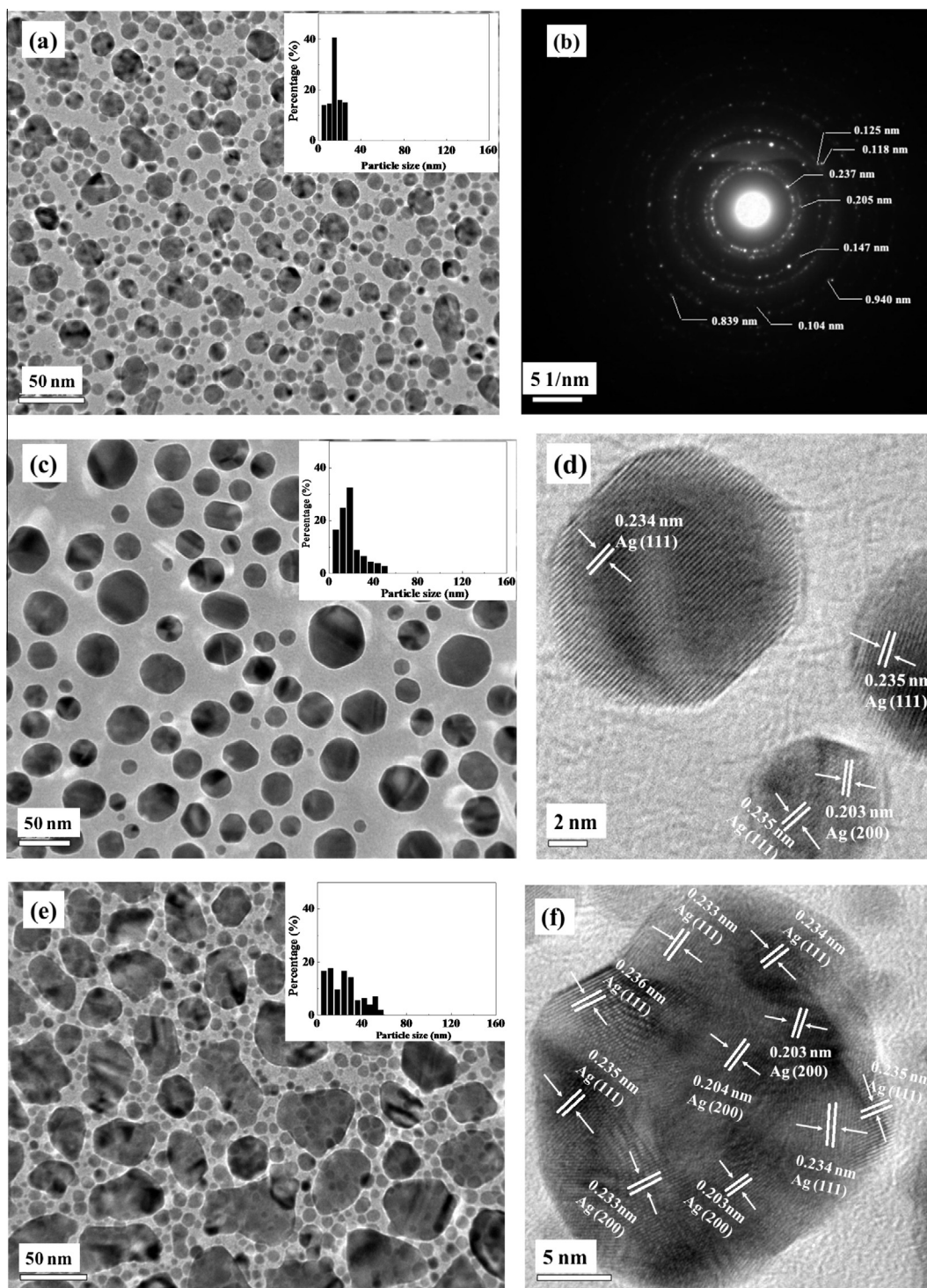


Fig. 2. TEM images of (a) Ag_{CA} , (c) Ag_{SDBS} , (e) Ag_{Tween} , (g) Ag_{DS} , and (i) Ag_{PVP} nanoparticles, HRTEM images of (d) Ag_{SDBS} and (f) Ag_{Tween} nanoparticles, and SAED patterns of (b) Ag_{CA} , (h) Ag_{DS} , and (j) Ag_{PVP} nanoparticles.

reaction temperatures. After reacting for 4 h under 1 MPa O_2 , the conversions of 1,2-propanediol increased from 30.8% to 94.9% with increasing the reaction temperatures from 80 to 140 °C. The selectivities of lactic acid increased from 41% to 62% with increasing the reaction temperature from 80 to 120 °C, and then decreased to 53.3% at 140 °C. The total selectivities of formic and acetic acids decreased from 59% to 38% with increasing the reaction temperatures from 80 to 120 °C, and then increased to 46.7% at 140 °C. The results indicated that increasing the reaction temperature

favorable the conversion of 1,2-propanediol to lactic acid. However, the oxidative cleavage of intermediates could rapidly occur at high reaction temperature, leading to the formation of more formic and acetic acids. Furthermore, it was also found that the 1,2-propanediol conversion rapidly increased with prolonging the reaction time, but the lactic acid selectivity slightly decreased. At the same time, the selectivities of formic and acetic acids slightly increased. It was suggested that the formation of lactic, formic, and acetic acids was probably parallel reactions.

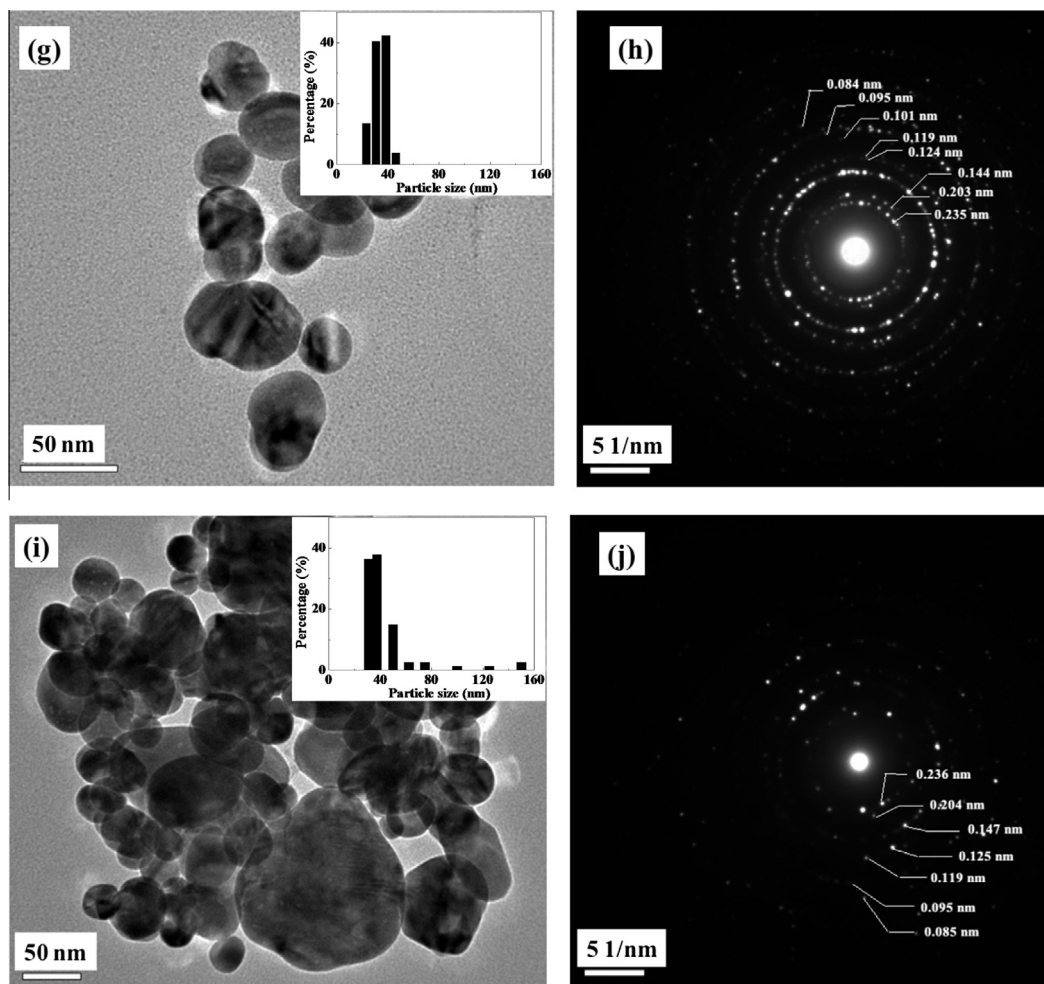


Fig. 2 (continued)

3.4.2. Effect of 1,2-propanediol concentration

The effect of 1,2-propanediol concentration on the catalytic oxidation of 1,2-propanediol over Ag_{Tween} nanoparticle catalyst is shown in Fig. 4. When the 1,2-propanediol concentrations increased from 0.14 to 0.56 mol L⁻¹, after reacting at 120 °C and 1 MPa O₂ for 4 h, the conversions of 1,2-propanediol decreased from 99.7% to 42.2%. The selectivities of lactic acid increased from 50.3% to 65.7%. The selectivities of formic acid and acetic acid were less than 17.1% and 32.6%, respectively. The lactic acid selectivity increased while the selectivities of acetic and formic acids decreased with increasing 1,2-propanediol concentration. It could be explained as that under low 1,2-propanediol concentration, more catalytic active sites available on the surfaces of the Ag_{Tween} nanoparticles led to the cleavage and oxidation of intermediates to form more formic and acetic acids.

3.4.3. Effect of O₂ pressure

When 1,2-propanediol was oxidized over Ag_{Tween} nanoparticle catalyst at O₂ pressures ranging from 0.5 to 2 MPa, after reacting at 120 °C for 4 h, the conversions of 1,2-propanediol increased from 55.3% to 87.6% (Fig. 5). The selectivities of lactic acid decreased from 64.2% to 45.8%. The total selectivities of formic acid and acetic acid increased to 54.2%. The results showed that high O₂ pressure was beneficial for the conversion of 1,2-propanediol due to more active oxygen available. However, the presence of more active oxygen gave low lactic acid selectivity due to the formation of more formic and acetic acids.

3.4.4. Effect of NaOH concentration

Fig. 6 shows the effect of NaOH concentration on the catalytic oxidation of 1,2-propanediol over Ag_{Tween} nanoparticles. The conversion of 1,2-propanediol was less than 1.5%, and no lactic, formic, and acetic acids were detected without NaOH. When the NaOH concentration was 0.28 mol L⁻¹, the 1,2-propanediol conversion of 58.3% and the selectivities of lactic, formic, and acetic acids of 31.2%, 24.8%, and 44.0% were obtained, respectively, after reacting at 120 °C for 4 h with 1 MPa O₂, indicating that alkaline surrounding was necessary for 1,2-propanediol conversion. While increasing the NaOH concentration to 0.56 mol L⁻¹, after reacting for 4 h, the 1,2-propanediol conversion and lactic acid selectivity increased to 65.6% and 62%, respectively, and the total formic and acetic acid selectivities decreased to 38%. High NaOH concentration favored the conversion of 1,2-propanediol to lactic acid. However, when the NaOH concentration was more than 0.56 mol L⁻¹, 1,2-propanediol conversion and product selectivities were similar to those with NaOH concentration of 0.56 mol L⁻¹.

3.4.5. Effect of catalyst loading

Fig. 7 shows the effect of catalyst loading on the catalytic oxidation of 1,2-propanediol over Ag_{Tween} nanoparticles. There was no conversion of 1,2-propanediol found without Ag_{Tween} nanoparticle catalyst. When the catalyst loadings were 0.03 and 0.06 g, after reacting at 120 °C for 4 h with 1 MPa O₂, the 1,2-propanediol conversions were 34.3% and 65.6%, respectively. The selectivities of lactic, formic, and acetic acids were 63.3%, 13.2%, and 23.5%;

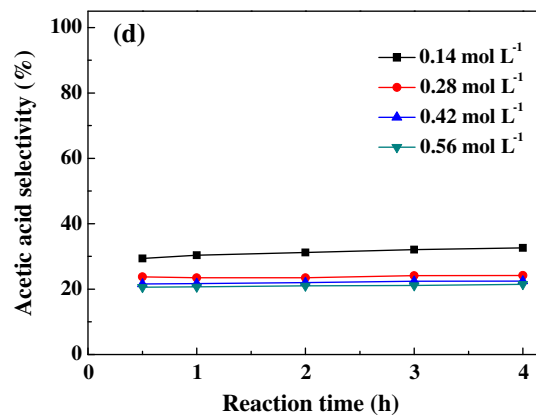
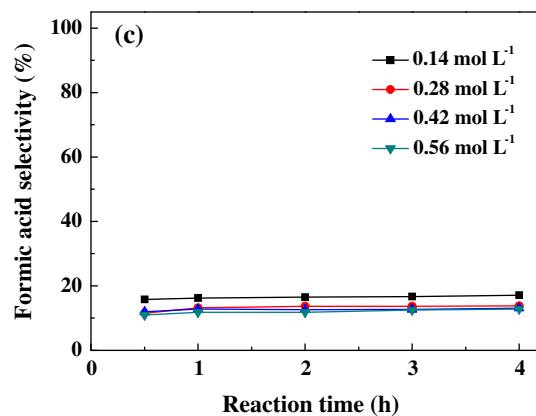
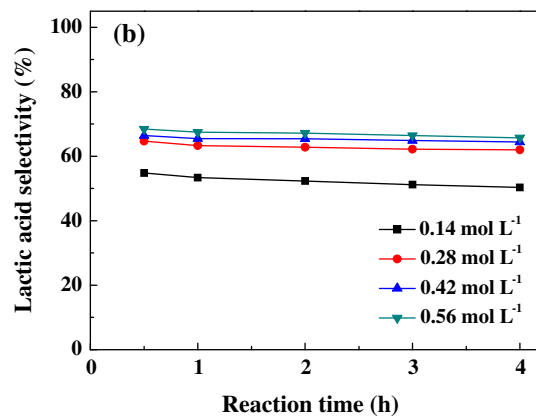
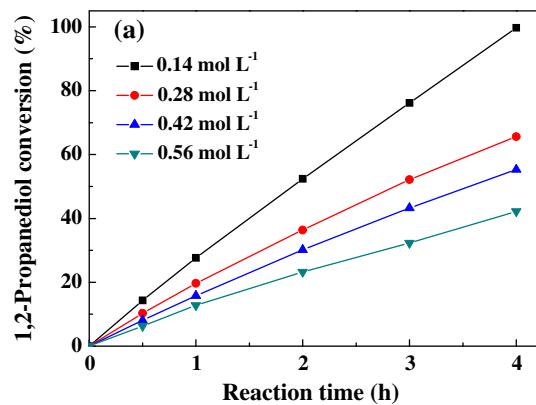
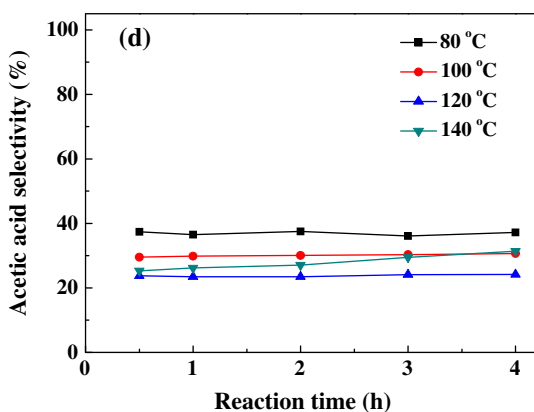
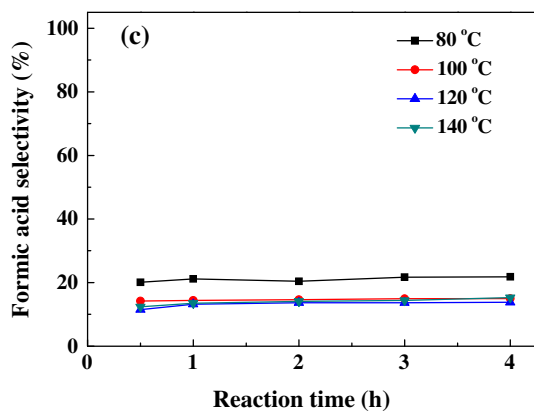
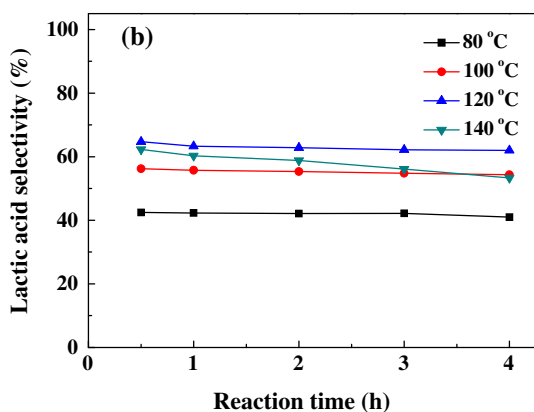
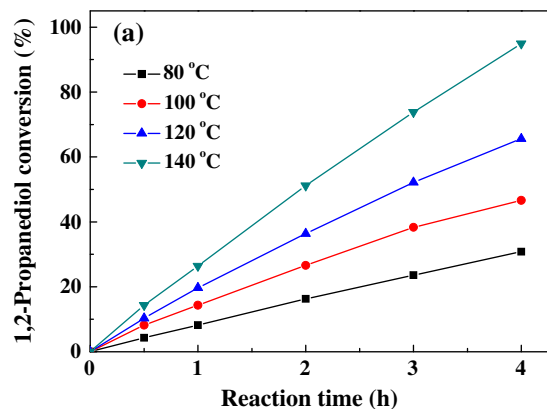


Fig. 3. Effect of reaction temperature on catalytic oxidation of 1,2-propanediol over Ag_{Tween} nanoparticles. Reaction conditions: 1,2-propanediol concentration, 0.28 mol L⁻¹; NaOH concentration, 0.56 mol L⁻¹; volume of solution, 200 mL; O₂ pressure, 1.0 MPa; catalyst loading, 0.06 g; and stirring rate, 600 rpm.

Fig. 4. Effect of 1,2-propanediol concentration on the catalytic oxidation of 1,2-propanediol over Ag_{Tween} nanoparticles. Reaction conditions: NaOH concentration, 0.56 mol L⁻¹; volume of solution, 200 mL; O₂ pressure, 1.0 MPa; reaction temperature, 120 °C; catalyst loading, 0.06 g; and stirring rate, 600 rpm.

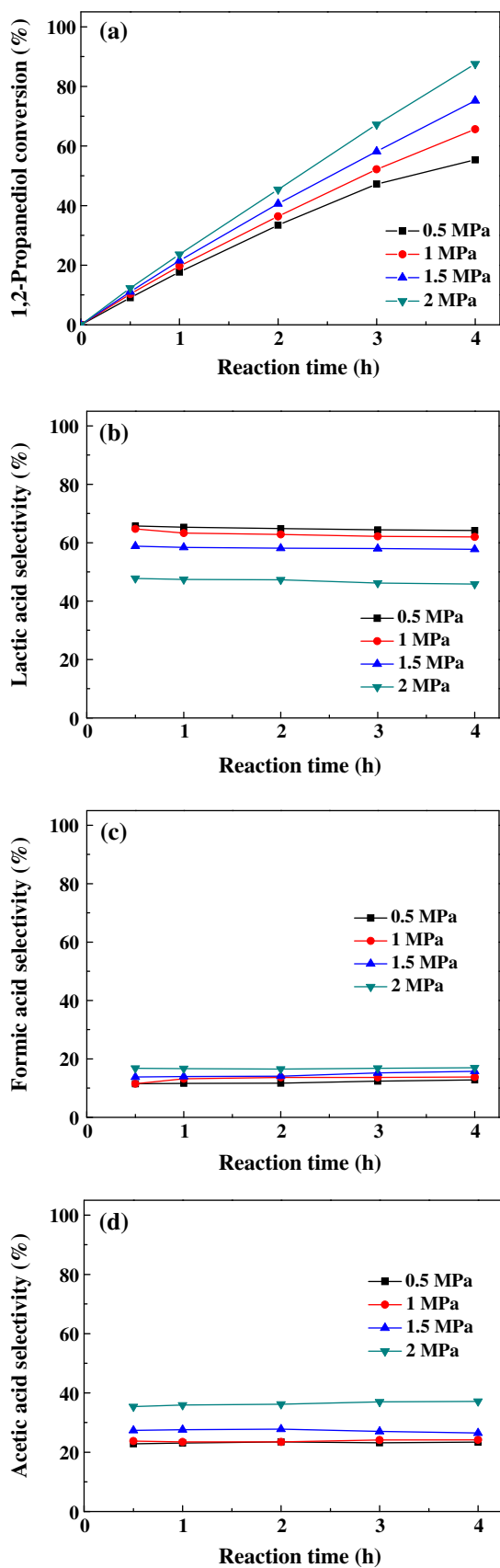


Fig. 5. Effect of O₂ pressure on the catalytic oxidation of 1,2-propanediol over Ag_{Tween} nanoparticles catalyst. Reaction conditions: 1,2-propanediol concentration, 0.28 mol L⁻¹; NaOH concentration, 0.56 mol L⁻¹; volume of solution, 200 mL; reaction temperature, 120 °C; catalyst loading, 0.06 g; and stirring rate, 600 rpm.

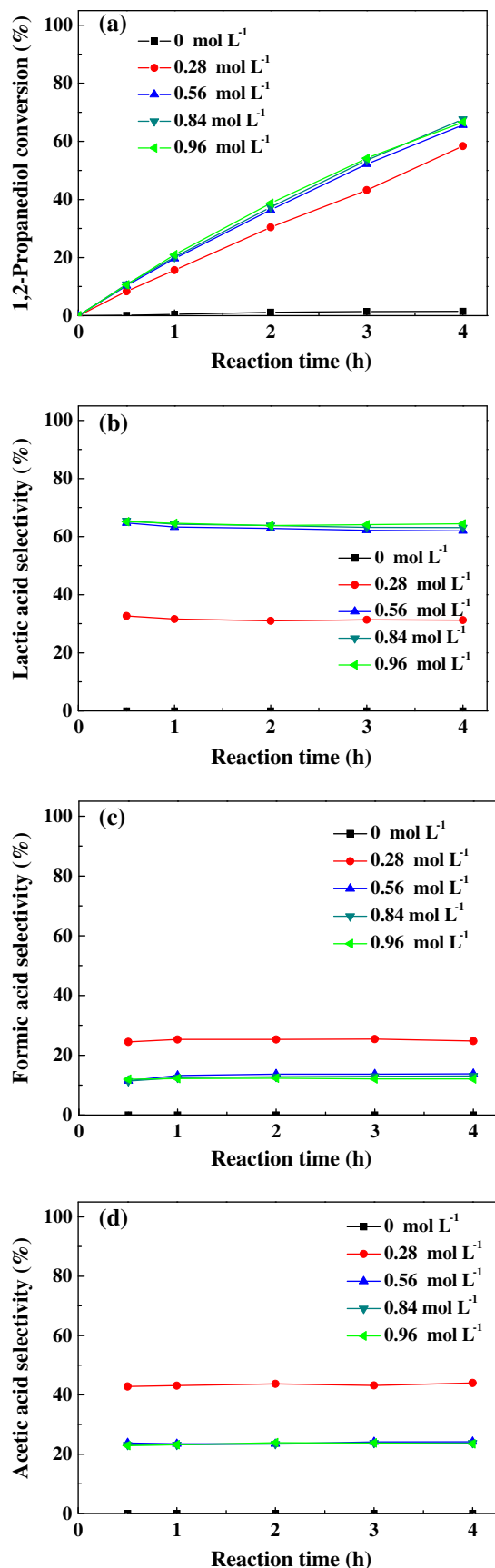


Fig. 6. Effect of NaOH concentration on catalytic oxidation of 1,2-propanediol over Ag_{Tween} nanoparticles catalysts. Reaction conditions: 1,2-propanediol concentration, 0.28 mol L⁻¹; volume of solution, 200 mL; O₂ pressure, 1.0 MPa; reaction temperature, 120 °C; catalyst loading, 0.06 g; and stirring rate, 600 rpm.

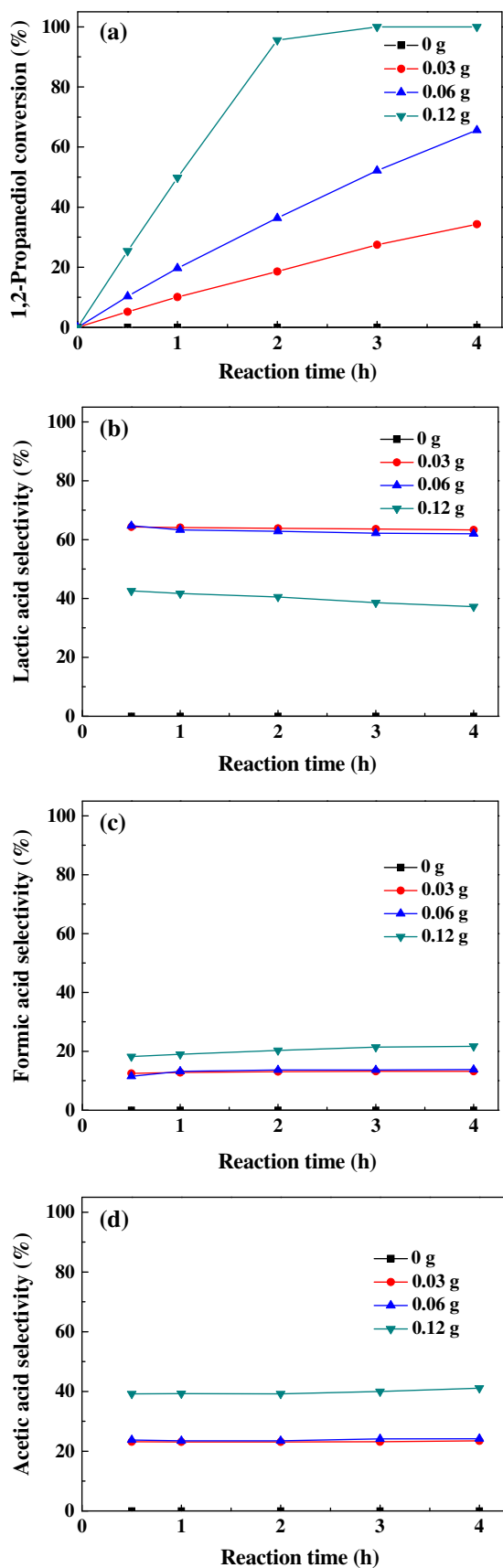


Fig. 7. Effect of catalyst loading on catalytic oxidation of 1,2-propanediol over Ag_{Tween} nanoparticles catalyst. Reaction conditions: 1,2-propanediol concentration, 0.28 mol L⁻¹; NaOH concentration, 0.56 mol L⁻¹; volume of solution, 200 mL; O₂ pressure, 1 MPa; reaction temperature, 120 °C; and stirring rate, 600 rpm.

62.0%, 13.8%, and 24.2%, respectively. With increasing the catalyst loading to 0.12 g, after reacting at 120 °C for 3 h, the 1,2-propanediol conversion reached 100%. The selectivities of lactic, formic, and acetic acids were 38.6%, 21.4%, and 40.0%, respectively. The selectivity of lactic acid with a high catalyst loading of 0.12 g was lower than those with low catalyst loadings of 0.03 and 0.06 g. The result showed that Ag nanoparticles not only catalyzed the conversion of 1,2-propanediol to lactic acid but also catalyzed the oxidation of intermediate to formic and acetic acids.

3.5. Catalytic oxidation of 1,2-propanediol to formic and acetic acids

Considering the spherical Ag_{CA} nanoparticle had high catalytic activity in the oxidation of 1,2-propanediol to formic and acetic acids, it was selected as the model catalyst to evaluate the effect of reaction parameter on the catalytic oxidation reaction. The results are showed in Fig. 8.

Fig. 8a shows the effect of reaction temperature on the catalytic oxidation of 1,2-propanediol over Ag_{CA} nanoparticles. The 1,2-propanediol conversions increased from 56.5% to 98.5% with increasing the reaction temperatures from 80 to 120 °C, after reacting for 3 h under 1 MPa O₂. The selectivities of formic and acetic acids increased from 26.6% to 30.5% and from 60.3% to 63.2%, respectively. The lactic acid selectivities decreased from 13.1% to 6.3% (Fig. S1). The results showed that high reaction temperature favored the conversion of 1,2-propanediol to formic and acetic acids other than lactic acid over Ag_{CA} nanoparticle catalyst. Furthermore, prolonging the reaction time could significantly enhance the 1,2-propanediol conversion. But the product selectivities were not obviously affected by prolonging the reaction time.

Fig. 8b shows the effect of 1,2-propanediol concentration on catalytic oxidation of 1,2-propanediol over Ag_{CA} nanoparticles. After reacting at 100 °C and 1 MPa O₂ for 3 h, with increasing the 1,2-propanediol concentrations from 0.14 to 0.42 mol L⁻¹, the 1,2-propanediol conversions decreased from 98.2% to 59.5%. The selectivities of formic and acetic acids decreased from 32.1% to 24.6% and from 65% to 59.2%, respectively. With increasing 1,2-propanediol concentration, the conversion of 1,2-propanediol and the selectivities of formic and acetic acids decreased.

Fig. 8c shows the effect of O₂ pressure on catalytic oxidation of 1,2-propanediol over Ag_{CA} nanoparticles. The 1,2-propanediol conversions and product selectivities were not obviously affected by varying the O₂ pressures from 0.5 to 1.5 MPa. The selectivities of formic, acetic, and lactic acids were ca. 30%, 61%, and 9%, respectively. It could be explained as that the adsorption of O₂ dissolved in the reaction solution on the surfaces of Ag_{CA} nanoparticles was probably saturated when the O₂ pressure was higher than 0.5 MPa. Further increasing O₂ pressure had no impact on the oxidation reaction.

3.6. Reaction kinetics

3.6.1. Preliminary consideration

A power-function type reaction kinetic equation was used to investigate the effect of 1,2-propanediol concentration, O₂ pressure, and reaction temperature on the reaction rate over Ag_{Tween} and Ag_{CA} nanoparticles. The effect of NaOH concentration on the reaction rate was ignored herein because the catalytic activities of the catalysts did not change when the NaOH concentration was more than 0.28 mol L⁻¹.

To eliminate the effect of diffusion, Ag_{Tween} nanoparticles with different loadings in the range of 0.03–0.12 g were used for the oxidation reaction of 1,2-propanediol with the concentration of 0.28 mol L⁻¹. A linear correlation between the catalyst loading and the conversion was observed at first 0.5 h (Fig. S2). According to Ref. [35], this result indicated that the initial

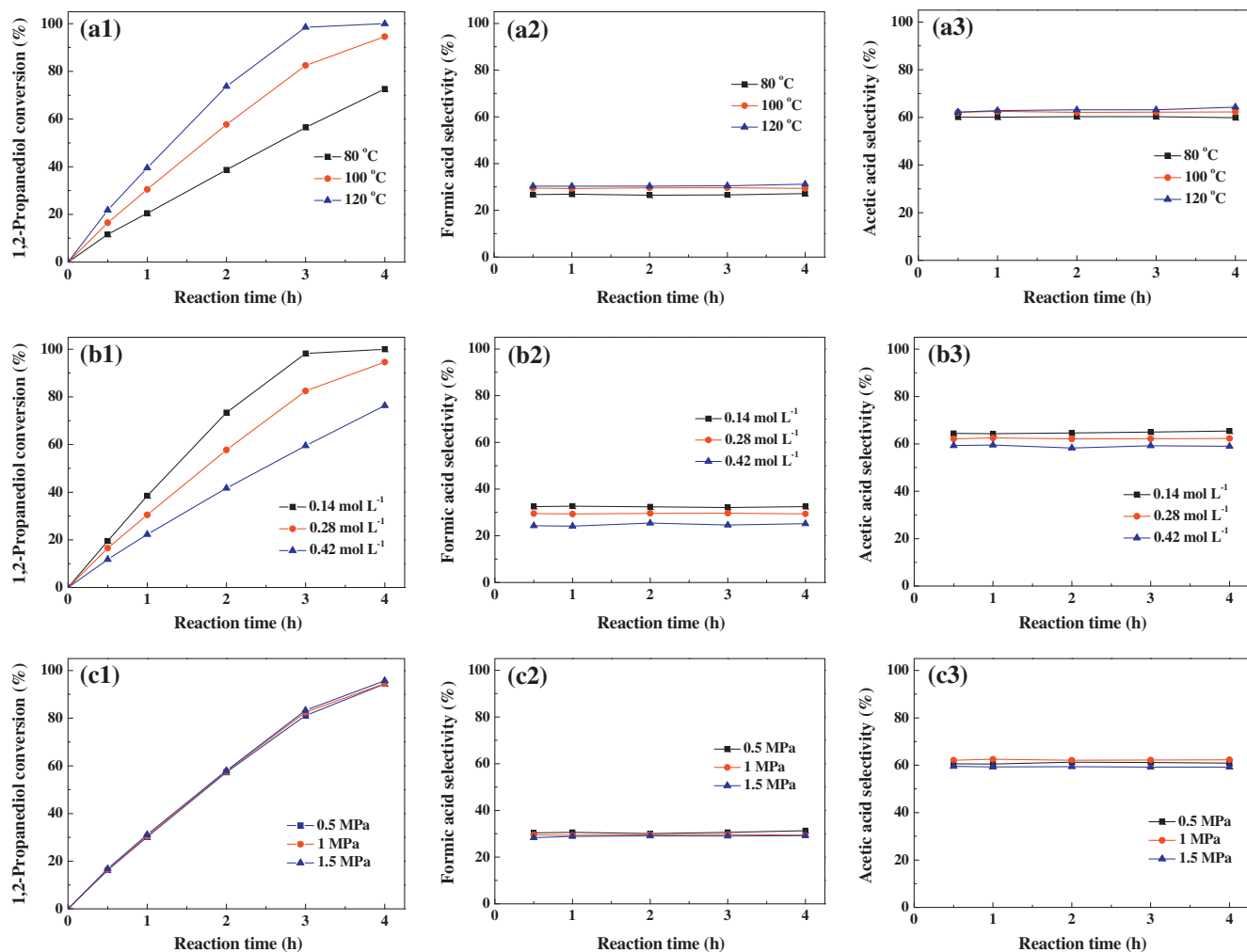


Fig. 8. Effect of (a) reaction temperature, (b) 1,2-propanediol concentration, and (c) O_2 pressure on catalytic oxidation of 1,2-propanediol over Ag_{CA} nanoparticles. Except for the varying reaction parameter, other fixed reaction parameters as follows: 1,2-propanediol concentration, 0.28 mol L^{-1} ; NaOH concentration, 0.56 mol L^{-1} ; volume of solution, 200 mL ; reaction temperature, $100 \text{ }^\circ\text{C}$; O_2 pressure, 1 MPa ; catalyst loading, 0.06 g ; and stirring rate, 600 rpm .

oxidation rate was controlled only by chemical reaction rather than mass diffusion.

The power-function type reaction kinetic equation is expressed as follows:

$$r = -dC_0/dt = kC_0^a P_0^b \quad (1)$$

where k is the rate constant. a and b are the reaction orders with respect to the 1,2-propanediol concentration and O_2 pressure. r is the initial reaction rate of 1,2-propanediol, $\text{mol L}^{-1} \text{ min}^{-1}$. C_0 is the initial concentration of 1,2-propanediol, mol L^{-1} . P_0 is the initial O_2 pressure, MPa. The rate constant k follows the Arrhenius equation.

$$k = A \exp(-E_a/RT) \quad (2)$$

where A is the pre-exponential factor and E_a is the activation energy, kJ mol^{-1} . R is the ideal gas constant, $8.314 \times 10^{-3} \text{ kJ mol}^{-1} \text{ K}^{-1}$. T is the reaction temperature, K.

3.6.2. Reaction order

A linear Eq. (3) is obtained by taking the natural logarithm of both sides of Eq. (1).

$$\ln r = \ln(-dC_0/dt) = \ln k + a \ln C_0 + b \ln P_0 \quad (3)$$

To calculate the reaction orders of a and b according to Eq. (3), the initial rates were calculated according to the data shown in Figs. 4a and 5a for Ag_{Tween} catalyst and Fig. 8b1 and c1 for Ag_{CA}

catalyst, respectively. The initial reaction rates of 1,2-propanediol under different reaction conditions were calculated at the first 0.5 h.

Fig. 9a shows the lines by plotting $\ln(-dC_0/dt)$ vs $\ln C_0$. The line for Ag_{Tween} catalyst was depicted according to the data shown in Fig. 4a while the line for Ag_{CA} catalyst was depicted according to the data shown Fig. 8b1. Two straight lines with the correlation coefficients of 0.9872 and 0.9708 were obtained, respectively. The corresponding slopes were 0.5 and 0.9, indicating that the reaction orders of 1,2-propanediol, a , were 0.5 and 0.9 over Ag_{Tween} and Ag_{CA} catalysts, respectively.

Fig. 9b shows the lines by plotting $\ln(-dP_0/dt)$ vs $\ln C_0$. The line for Ag_{Tween} catalyst was depicted according to the data shown in Fig. 5a while the line for Ag_{CA} catalyst was depicted according to the data shown Fig. 8c1. Two straight lines with the correlation coefficients of 0.9847 and 0.9704 were obtained, respectively. The corresponding slopes were 0.2 and 0.02, indicating that the reaction orders of O_2 pressure, b , were 0.2 and 0 over Ag_{Tween} and Ag_{CA} catalysts, respectively.

3.6.3. Activation energy

Combined with Eqs. (2) and (1) can be written as follows:

$$r = -dC_0/dt = A \exp(-E_a/RT) C_0^a P_0^b \quad (4)$$

Eq. (4) can be rearranged as follows:

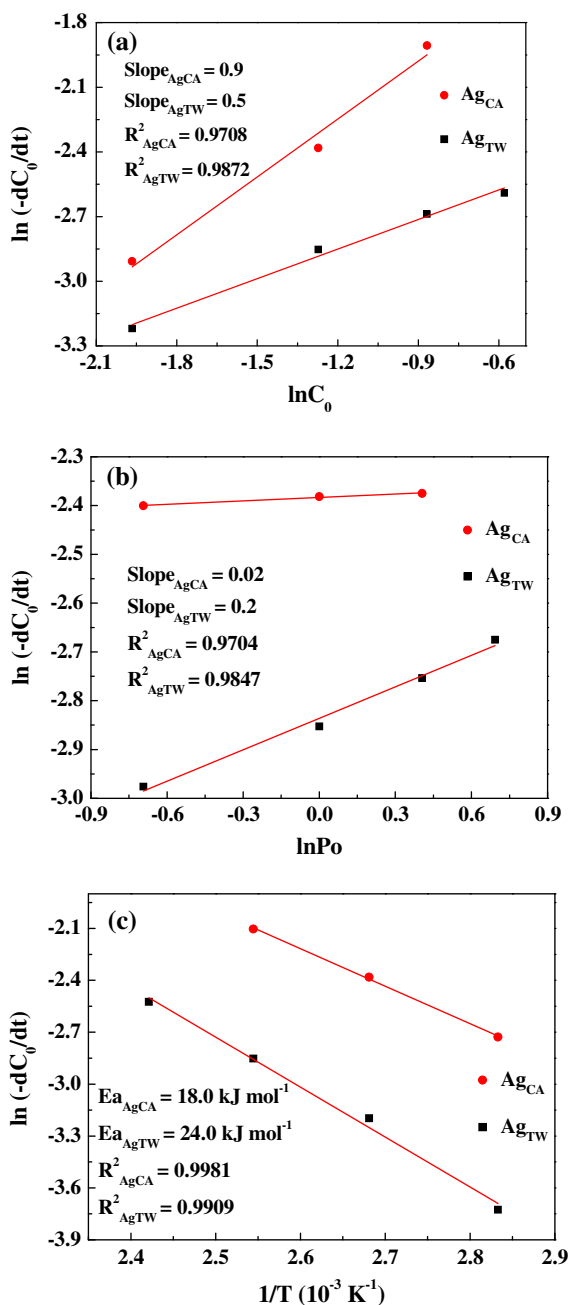


Fig. 9. Estimation of (a and b) the reaction orders and (c) the reaction activation energies for the power-function type reaction kinetics over Ag_{TWEEN} and Ag_{CA} catalysts.

$$\ln r = \ln(-dC_0/dt) = \ln(AC_0^a P_0^b) - (E_a/R)(1/T) \quad (5)$$

The reaction rates, r , at different reaction temperatures were calculated by using the data shown in Fig. 3a for Ag_{TWEEN} catalyst and the data shown in Fig. 8a1 for Ag_{CA} catalyst. According to Eq. (5), while plotting $\ln r$ vs $1/T$, two straight lines with good linear correlations of 0.9909 and 0.9981 were obtained, respectively (Fig. 9c). The values of reaction activation energy, E_a , were 24.0 and 18.0 kJ mol^{-1} over Ag_{TWEEN} and Ag_{CA} catalysts, respectively. The corresponding A values were 168 and 96. Over Ag_{TWEEN} and Ag_{CA} catalysts, their reaction kinetics were listed as follows:

$$r = -dC_0/dt = 168 \exp(-24/RT) C_0^{0.5} P_0^{0.2} \text{ mol L}^{-1} \text{ h}^{-1} \quad (6)$$

$$r = -dC_0/dt = 96 \exp(-18/RT) C_0^{0.9} \text{ mol L}^{-1} \text{ h}^{-1} \quad (7)$$

The activation energy over Ag_{TWEEN} catalyst was higher than that over Ag_{CA} catalyst. The frequency factor over Ag_{TWEEN} catalyst was also higher than that over Ag_{CA} catalyst. Furthermore, the reaction orders of 1,2-propanediol and O_2 pressure over Ag_{TWEEN} catalyst were different from those over Ag_{CA} catalyst. It could be explained as that the particle sizes of Ag nanoparticles significantly affected their catalytic activities.

3.7. Catalyst recycling performance

The recycling performances of Ag_{TWEEN} and Ag_{CA} catalysts for the catalytic oxidation of 1,2-propanediol are shown in Table 2. After reacting at 120 °C for 4 h, the catalysts were centrifugated and washed with distilled water and anhydrous ethanol before next recycling. For the fresh Ag_{TWEEN} catalyst, the conversion of 1,2-propanediol was 65.6% and the selectivities of lactic acid were 62%. After recycling for 5 times, the conversion of 1,2-propanediol and the selectivities of lactic acid were 59.7% and 59.5%, respectively. The results showed that the spent Ag_{TWEEN} catalyst had good recycling performance for the catalytic conversion of 1,2-propanediol to lactic acid. For the fresh Ag_{CA} catalyst, the conversion of 1,2-propanediol was 100% and the selectivities of formic and acetic acids were 30.5% and 63.2%, respectively. After recycling 5 times, the 1,2-propanediol conversion was 100% and the selectivities of formic and acetic acids were 29.9% and 63.3%, respectively. The spent Ag_{CA} catalyst had good recycling performance for the catalytic conversion of 1,2-propanediol to formic and acetic acids.

3.8. Reaction mechanism

To examine the effect of substrate structure on reactivity, the simple diols (1,2-propanediol and ethylene glycol) and monohydric alcohols (propanol, ethanol, and methanol) were oxidized with O_2 over Ag_{TWEEN} and Ag_{CA} catalysts, respectively, at 120 °C and 1 MPa O_2 for 4 h. The results are listed in Table 3. For the oxidation of 1,2-propanediol, high selectivities of lactic acid and formic and acetic acids were observed when the reaction was catalyzed by Ag_{TWEEN} and Ag_{CA} catalysts, respectively. For the oxidation of ethylene glycol, glycolic acid was the sole product observed when using Ag_{TWEEN} and Ag_{CA} nanoparticles as catalyst, respectively. For the oxidation of monohydric alcohols, such as 1-propanol, 2-propanol, ethanol, and methanol, no conversion was found when Ag_{TWEEN} or Ag_{CA} nanoparticles were used as the catalysts. The results indicated that diols were more reactive than monohydric alcohols over Ag nanoparticle catalysts due to that the vicinal diol structure would be much more capable of forming a complex with the metallic

Table 2

Recycling performances of Ag_{TWEEN} and Ag_{CA} catalysts for catalytic oxidation of 1,2-propanediol.^a

Catalysts	Recycling time	1,2-propanediol conversions (%)	Selectivities (%)		
			Lactic acid	Formic acid	Acetic acid
Ag_{TWEEN}	1	65.6	62.0	13.8	24.2
	2	64.8	61.2	14.1	24.7
	3	63.0	61	13.9	25.1
	4	61.6	60	14.4	25.6
	5	59.7	59.5	14.3	26.2
Ag_{CA}	1	100	6.3	30.5	63.2
	2	100	6.1	30.3	63.6
	3	100	6.5	30.8	62.7
	4	100	5.9	31.1	63.0
	5	100	6.8	29.9	63.3

^a Reaction conditions: 1,2-propanediol concentration, 0.28 mol L^{-1} ; NaOH concentration, 0.56 mol L^{-1} ; volume of solution, 200 mL; catalyst, 0.06 g; reaction temperature, 120 °C; reaction time, 4 h; and stirring rate, 600 rpm.

Table 3
Oxidation of alcohols and possible intermediates catalyzed by Ag_{Tween} and Ag_{CA} nanoparticle catalysts.

Substrates	Catalysts	Conversions (%)	Selectivities (%)
1,2-propanediol ^a	Ag _{Tween}	65.6	62.0 (lactic acid), 13.8 (formic acid), and 24.2 (acetic acid)
	Ag _{CA}	100	6.3 (lactic acid), 30.5 (formic acid), and 63.2 (acetic acid)
Ethylene glycol ^a	Ag _{Tween}	66.7	100 (glycolic acid)
	Ag _{CA}	89.4	100 (glycolic acid)
1-Propanol ^a	Ag _{Tween}	0	0
	Ag _{CA}	0	0
2-Propanol ^a	Ag _{Tween}	0	0
	Ag _{CA}	0	0
Ethanol ^a	Ag _{Tween}	0	0
	Ag _{CA}	0	0
Methanol ^a	Ag _{Tween}	0	0
	Ag _{CA}	0	0
Acetaldehyde ^b	Ag _{Tween}	100	100 (acetic acid)
	Ag _{CA}	100	100 (acetic acid)
Formaldehyde ^b	Ag _{Tween}	100	100 (formic acid)
	Ag _{CA}	100	100 (formic acid)
Hydroxyacetone ^b	Ag _{Tween}	100	46.3 (lactic acid), 17.5 (formic acid), and 38.2 (acetic acid)
	Ag _{CA}	100	38.6 (lactic acid), 20.2 (formic acid), and 41.2 (acetic acid)
Pyruvaldehyde ^b	Ag _{Tween}	100	71.6 (lactic acid), 9.3 (formic acid), and 19.1 (acetic acid)
	Ag _{CA}	100	48.4 (lactic acid), 17.1 (formic acid), and 34.5 (acetic acid)
Lactic acid ^b	Ag _{Tween}	0.8	0
	Ag _{CA}	1.1	0

^a Reaction conditions: substrate, 0.28 mol L⁻¹; NaOH, 0.56 mol L⁻¹; volume of solution, 200 mL; catalyst loading, 0.06 g; reaction temperature, 120 °C; O₂ pressure, 1 MPa; reaction time, 4 h; and stirring rate, 600 rpm.

^b Reaction conditions: substrate, 0.28 mol L⁻¹; NaOH, 0.56 mol L⁻¹; volume of solution, 200 mL; catalyst loading, 0.06 g; reaction temperature, 120 °C; O₂ pressure, 1 MPa; reaction time, 0.5 h; and stirring rate, 600 rpm.

catalyst surface, which could facilitate the oxidation [23,26]. No ethanol, methanol, and glycolic acid were detected (Table 3) in the oxidation of 1,2-propanediol, indicating that 1,2-propanediol could not be cleaved to ethanol, methanol, and ethylene glycol over Ag nanoparticle catalysts. Furthermore, the carbon mole ratios of the resultant acetic acid to formic acid were close to 2:1 in all our experiments, indicating that the acetic acid and formic acid were derived from a C₃ intermediate in the oxidation of 1,2-propanediol. Table 3 shows that over Ag_{Tween} and Ag_{CA} catalysts, formaldehyde and acetaldehyde were rapidly and completely oxidized to formic acid and acetic acid, respectively, indicating that the formation of formic and acetic acids was possibly derived from

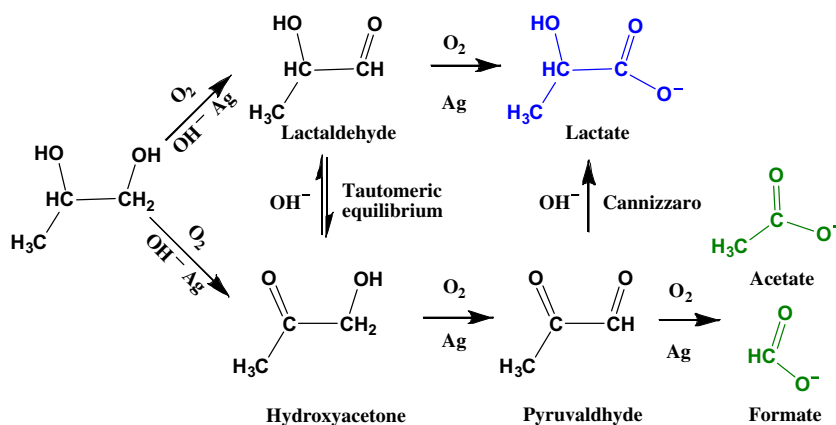
the oxidation of formaldehyde and acetaldehyde, which were formed via the cleavage of pyruvaldehyde.

It was reported that there involved two possible parallel pathways for the catalytic oxidation of 1,2-propanediol as shown in Scheme 1 [23,27,28]. If the oxidation of the primary hydroxyl group occurs, 1,2-propanediol can be oxidized to lactaldehyde, which can be rapidly oxidized to lactic acid because lactaldehyde is not detected under our present experimental conditions. If the oxidation of secondary hydroxyl group occurs, 1,2-propanediol can be oxidized to hydroxyacetone. The resultant hydroxyacetone can be oxidized to pyruvaldehyde, which can be further oxidized and cleaved to acetic acid and formic acid [23,29]. Meanwhile, hydroxyacetone can be transformed to lactaldehyde via the tautomeric equilibrium. Then, the resultant lactaldehyde is oxidized to lactic acid. Pyruvaldehyde can also be converted to lactate in an alkaline solution through the Cannizzaro reaction.

We also detected the catalytic activities of Ag_{Tween} or Ag_{CA} nanoparticles for the oxidation of hydroxyacetone, pyruvaldehyde, and lactic acid (Table 3). It was found that both hydroxyacetone and pyruvaldehyde could be rapidly oxidized to lactic, formic, and acetic acids. Ag_{Tween} nanoparticles had higher catalytic activity for the formation of lactic acid than Ag_{CA} nanoparticles. However, both catalysts had no catalytic activity for the oxidation of lactic acid. Furthermore, in the absence of NaOH or Ag nanoparticle catalyst, 1,2-propanediol was hardly oxidized (Figs. 6 and 7). The results implied that Ag nanoparticles and alkali could rapidly cocatalyze the oxidation of 1,2-propanediol to lactaldehyde, hydroxyacetone, and pyruvaldehyde. Then, the resultant intermediates could be rapidly oxidized to form lactic, formic, and acetic acids. Small-sized Ag_{CA} nanoparticles favored the oxidation of pyruvaldehyde to formic and acetic acids as compared to the large-sized Ag_{Tween} nanoparticles. In fact, Ag_{Tween} and Ag_{SDBS} nanoparticles gave high lactic acid selectivity among the Ag nanoparticle catalysts. Ag_{DS} and Ag_{PVP} nanoparticles with larger particle sizes gave low 1,2-propanediol conversion and low lactic acid selectivity. The particle size of Ag nanoparticles played an important role in the selectively catalytic oxidation of 1,2-propanediol.

4. Conclusions

Spherical Ag nanoparticles with particle sizes in the range of 15.2–43.8 nm were prepared by chemical reduction method with different-structured organic modifiers. The Ag_{Tween} nanoparticles with the average particle size of 25.3 nm selectively catalyzed 1,2-propanediol to lactic acid in NaOH solution with the selectivity of 62.0% at the 1,2-propanediol conversion of 65.6% after reacting



Scheme 1. Reaction routes in the oxidation of 1,2-propanediol to lactic, formic, and acetic acids catalyzed by Ag nanoparticle catalysts [23,27,28].

for 4 h at 120 °C under 1.0 MPa O₂, while the Ag_{CA} nanoparticles with the average particle size of 15.2 nm selectively catalyzed 1,2-propanediol to formic and acetic acids with the selectivities of 30.5% and 63.2%, respectively, at complete 1,2-propanediol conversion. The reaction kinetics for the catalytic oxidation of 1,2-propanediol over Ag_{rween} nanoparticles was different from that over Ag_{CA} nanoparticles, probably due to their size effect. The Ag nanoparticle catalysts had good recycling performance. Effective oxidation of sustainable 1,2-propanediol over Ag nanoparticle catalysts is an alternative method for selective, facile, and eco-friendly production of lactic, formic, and acetic acids.

Acknowledgments

The authors sincerely thank Professor K. Chen (Jiangsu University) for supporting the TEM and HRTEM measurements. This work was financially supported by research funds from Jiangsu Province Education Bureau (No. 11KJB530002), Jiangsu University for Young Researchers (Nos. 11JDG028, 2010-4849), China Postdoctoral Foundation Committee (No. 2011M500866), and Ph.D. Innovation Programs Foundation of Jiangsu Province (No. CXZZ13_0666).

Appendix A. Supplementary material

Supplementary data associated with this article can be found, in the online version, at <http://dx.doi.org/10.1016/j.jcat.2015.03.009>.

References

- [1] H.M. Ijmker, M. Gramblička, S.R.A. Kersten, A.G.J. van der Ham, B. Schuur, *Sep. Sci. Technol.* 125 (2014) 256–263.
- [2] F.E. Paulik, J.F. Roth, *Chem. Commun.* (1968) 1578.
- [3] A. García-Trenco, A. Martínez, *Catal. Today* 215 (2013) 152–161.
- [4] F.G. Üçtuğ, S. Ağralı, Y. Arıkan, E. Avcioğlu, *J. Environ. Manage.* 132 (2014) 1–8.
- [5] G. Prieto, J.D. Meeldijk, K.P. de Jong, P.E. de Jongh, *J. Catal.* 303 (2013) 31–40.
- [6] K.X. Wang, H.F. Xu, W.S. Li, C.T. Au, X.P. Zhou, *Appl. Catal. A: Gen.* 304 (2006) 168–177.
- [7] X.B. Li, E. Iglesia, *Appl. Catal. A: Gen.* 334 (2008) 339–347.
- [8] R.G. Zhang, L.Z. Song, H.Y. Liu, B.J. Wan, *Appl. Catal. A: Gen.* 443–444 (2012) 50–58.
- [9] K.X. Wang, H.F. Xu, W.S. Li, X.P. Zhou, *J. Mol. Catal. A: Chem.* 225 (2005) 65–69.
- [10] H.R. Arandjyan, M. Parvari, *J. Nat. Gas Chem.* 7 (2008) 213–224.
- [11] T. Ghaffar, M. Irshad, Z. Anwar, T. Aqil, Z. Zulfiqar, A. Tariq, M. Kamran, N. Ehsan, S. Mehmood, *J. Radiat. Res. Appl. Sci.* 7 (2014) 222–229.
- [12] Y.J. Wee, J.N. Kim, H.W. Ryu, *Food Technol. Biotechnol.* 44 (2006) 163–172.
- [13] M.A. Randhawa, A. Ahmed, K. Akram, *Pakistan J. Botany* 44 (2012) 333–338.
- [14] F. Carrasco, J. Cailloux, P.E. Sánchez-Jiménez, M.L. Maspocho, *Polym. Degrad. Stab.* 104 (2014) 40–49.
- [15] J. Sikder, S. Chakraborty, P. Pala, E. Driolic, C. Bhattacharjee, *Biochem. Eng. J.* 69 (2012) 130–137.
- [16] J.G. van Bennekom, R.H. Venderbosch, D. Assink, K.P.J. Lemmens, H.J. Heeres, *Chem. Eng. J.* 207–208 (2012) 245–253.
- [17] A. Bienholz, H. Hofmann, P. Claus, *Appl. Catal. A: Gen.* 391 (2011) 153–157.
- [18] M. Besson, P. Gallezot, C. Pinel, *Chem. Rev.* 114 (2014) 1827–1870.
- [19] L. Zhao, J.H. Zhou, Z.J. Sui, X.G. Zhou, *Chem. Eng. Sci.* 65 (2010) 30–35.
- [20] Y. Feng, H. Yin, A. Wang, L. Shen, L. Yu, T. Jiang, *Chem. Eng. J.* 168 (2011) 403–412.
- [21] Y. Feng, H. Yin, L. Shen, A. Wang, Y. Shen, T. Jiang, *Chem. Eng. Tech.* 36 (2013) 73–82.
- [22] L. Prati, M. Rossi, *J. Catal.* 176 (1998) 552–560.
- [23] N. Dimitratos, J.A. Lopez-Sanchez, S. Meenakshisundaram, J.M. Anthonykutti, G. Brett, A.F. Carley, S.H. Taylor, D.W. Knight, G.J. Hutchings, *Green Chem.* 11 (2009) 1209–1216.
- [24] Y. Ryabenkova, P.J. Miedziak, N.F. Dummer, S.H. Taylor, N. Dimitratos, D.J. Willock, D. Bethell, D.W. Knight, G.J. Hutchings, *Top Catal.* 55 (2012) 1283–1288.
- [25] Y. Ryabenkova, Q. He, P.J. Miedziak, N.F. Dummer, S.H. Taylor, A.F. Carley, D.J. Morgan, N. Dimitratos, D.J. Willock, D. Bethell, D.W. Knight, D. Chadwick, C.J. Kiely, G.J. Hutchings, *Catal. Today* 203 (2013) 139–145.
- [26] M.B. Griffin, A.A. Rodriguez, M.M. Montemore, J.R. Monnier, C.T. Williams, J.W. Medlin, *J. Catal.* 307 (2013) 111–120.
- [27] Y.H. Feng, H.B. Yin, D.Z. Gao, A.L. Wang, L.Q. Shen, M.J. Meng, *J. Catal.* 316 (2014) 67–77.
- [28] Y.H. Feng, H.B. Yin, A.L. Wang, D.Z. Gao, X.Y. Zhu, L.Q. Shen, M.J. Meng, *Appl. Catal. A: Gen.* 482 (2014) 49–60.
- [29] H. Ma, X. Nie, J.Y. Cai, C. Chen, J. Gao, H. Miao, J. Xu, *Sci. China Chem.* 53 (2010) 1497–1501.
- [30] H.H.C.M. Pinxt, B.F.M. Kuster, G.B. Marin, *Appl. Catal. A: Gen.* 191 (2000) 45–54.
- [31] H.M. Amin, A.M. Hashem, M.S. Ashour, R. Hatti-Kaul, *J. Genet. Eng. Biotechnol.* 11 (2013) 53–59.
- [32] <http://www.docin.com/p-445508830.html>.
- [33] <http://mcgroup.co.uk/news/20140418/propylene-glycol-market-reach-supplydem-and-balance-2015.html>.
- [34] B.M. Bhanage, S. Fujita, Y. Ikushima, M. Arai, *Green Chem.* 5 (2003) 429–432.
- [35] X. Huang, X. Wang, X. Wang, X. Wang, M. Tan, W. Ding, X. Lu, *J. Catal.* 301 (2013) 217–226.